

Title	Spatial analysis of failure sites in large area MIM capacitors using wavelets
Authors	Muñoz-Gorritz, J.; Monaghan, Scott; Cherkaoui, Karim; Suñé, Jordi; Hurley, Paul K.; Miranda, Enrique
Publication date	2017-04-13
Original Citation	Muñoz-Gorritz, J., Monaghan, S., Cherkaoui, K., Suñé, J., Hurley, P. K. and Miranda, E. (2017) 'Spatial analysis of failure sites in large area MIM capacitors using wavelets', Microelectronic Engineering, 178, pp. 10-16. doi:10.1016/j.mee.2017.04.011
Type of publication	Article (peer-reviewed)
Link to publisher's version	10.1016/j.mee.2017.04.011
Rights	© 2017 Published by Elsevier B.V. This manuscript version is made available under the CC-BY-NC-ND 4.0 license. - https://creativecommons.org/licenses/by-nc-nd/4.0/
Download date	2023-05-05 20:20:14
Item downloaded from	http://hdl.handle.net/10468/3957

Accepted Manuscript

Spatial analysis of failure sites in large area MIM capacitors using wavelets

J. Muñoz-Gorriz, S. Monaghan, K. Cherkaoui, J. Suñé, P.K. Hurley, E. Miranda



PII: S0167-9317(17)30139-9
DOI: doi: [10.1016/j.mee.2017.04.011](https://doi.org/10.1016/j.mee.2017.04.011)
Reference: MEE 10516

To appear in: *Microelectronic Engineering*

Received date: 20 February 2017
Revised date: 1 April 2017
Accepted date: 11 April 2017

Please cite this article as: J. Muñoz-Gorriz, S. Monaghan, K. Cherkaoui, J. Suñé, P.K. Hurley, E. Miranda, Spatial analysis of failure sites in large area MIM capacitors using wavelets. The address for the corresponding author was captured as affiliation for all authors. Please check if appropriate. Mee(2017), doi: [10.1016/j.mee.2017.04.011](https://doi.org/10.1016/j.mee.2017.04.011)

This is a PDF file of an unedited manuscript that has been accepted for publication. As a service to our customers we are providing this early version of the manuscript. The manuscript will undergo copyediting, typesetting, and review of the resulting proof before it is published in its final form. Please note that during the production process errors may be discovered which could affect the content, and all legal disclaimers that apply to the journal pertain.

Spatial analysis of failure sites in large area MIM capacitors using wavelets

J. Muñoz-Gorriz¹, S. Monaghan², K. Cherkaoui², J. Suñé¹, P.K. Hurley²,
E. Miranda¹

¹Departament d'Enginyeria Electrònica, Universitat Autònoma de Barcelona,
Spain

²Tyndall National Institute, University College Cork, Cork, Ireland
E-mail address of corresponding author: enrique.miranda@uab.cat

Abstract

The spatial distribution of failure sites in large area (10^4 - 10^5 μm^2) metal-insulator-metal (MIM) capacitors with high- K dielectric (HfO_2) is investigated using angular wavelets. The failure sites are the consequence of constant or ramped electrical stress applied on the capacitors. Because of the important local thermal effects that take place during stress, the failure sites become visible as a point pattern on the top metal electrode. In case of less damaged devices, the results obtained with the wavelet variance method are consistent with an isotropic distribution of breakdown spots as expected for a Poisson point process (complete spatial randomness). On the contrary, for severely damaged devices, the method shows signs of preferred directions of degradation related to the voltage probe location. In this case, the anisotropy is confirmed by alternative spatial statistics

methods such as the angular point-to-event distribution and the pair correlation function.

Keywords: oxide breakdown; reliability, MIM, spatial statistics

1. Introduction

Wavelet method is widely used in mathematics and engineering for signal processing and data compression [1]. However, to our knowledge, it has never been applied to an oxide reliability problem such as the spatial distribution of breakdown (BD) spots in MIM capacitors. On the contrary, the wavelet method for point pattern analysis is often used to investigate geographical and ecological spatial data [2]. In a previous paper [3], we studied the distribution of failure sites in severely damaged MIM devices but following more conventional approaches including distance and angular histograms [4]. Although angular histogram methods provide relevant information about the spatial distribution of BD spots, the analysis frequently relies on a particular focal point, and therefore are not global in essence (information averaged across all possible focal points) as expected in spatial statistics.

The failure sites investigated in this work are the consequence of constant or ramped electrical stress applied on the capacitors. Because of the huge thermal effects associated with the generation of shorts across the oxide film during stress, the damage become visible as a mark pattern on the top metal electrode. The effects of similar discharge transients on the gate electrode of MIS devices have also been described in [5]. From the microscopic viewpoint, the occurrence of a

failure event corresponds to the local accumulation of defects and the formation of a percolation path spanning the dielectric material [6]. The final result of this electrothermal process is the appearance of multiple crater-like structures with typical sizes in the μm range like the one shown in Fig. 1. These structures are often referred to as hard BDs with lateral propagation. The catastrophic events are at the end the consequence of micro-explosions accompanied by the local melting and evaporation of the metal electrode. Images obtained by transient infrared thermography reveal that some of the failure sites remain conducting after the occurrence of the micro-explosions while others, just leave their fingerprints on the electrode material remaining inactive throughout the experiment [7]. This latest behaviour indicates the local absence of the electrode material, which is typical of the self-healing process that can take place in metallized film capacitors [8].

In this work, the angular distribution of the kind of failure events discussed above was investigated. The obtained results using the wavelet variance method indicate isotropic BD spot distributions in agreement with what is expected for a Poisson point process or Complete Spatial Randomness (CSR) [4]. However, for severely damaged devices (long stress times and consequently large number of BD spots), the angular information displays some particular features that can be linked to preferred directions of degradation related to the voltage probe location. In this method, no focal point (a particular point of the process or special location) needs to be considered *a priori*, which is a crucial issue when no information is available on the position of the source of degradation. All points in a predefined area are

equally treated as focal points. It is worth mentioning that the technique of wavelets applied to the assessment of isotropy or to the identification of preferred directions might have a broader range of application other than the one reported here: defects in polycrystalline and ferroelectric films, dislocations and impurities in solar panels, metallized film capacitors, etc [8-10].

2. Devices and experimental setup

The devices investigated in this work are MIM capacitors with HfO_2 (30 nm-thick) as the dielectric and Pt electrodes. The area of the devices ranges from 10^4 to $10^5 \mu\text{m}^2$. The capacitors were fabricated onto a 200 nm-thick thermal SiO_2 layer grown on n-type Si (100) substrates with resistivities of 1-4 $\Omega\cdot\text{cm}$. First, a 200 nm thick Pt layer was deposited by electron-beam evaporation. A 30 nm-thick HfO_2 layer was then deposited by a Cambridge NanoTech Fiji atomic layer deposition (ALD) system using TEMAHf precursor and H_2O . After this, a 200 nm-thick Pt layer was deposited on top of the HfO_2 layer. Lithography and lift-off processes were used to form arrays of capacitors with different sizes. The access to the bottom Pt electrode was enabled via dry etching technique using a mask/resist process that removes the HfO_2 to the bottom Pt metal while at the same time protecting the top Pt electrode of the patterned devices. In our capacitors, the oxide layer extends 25 μm beyond the perimeter edge of the top metal. In order to generate the BD spots, the devices were subjected to ramped (typically 0V \rightarrow 12V) or constant (typically 9V for 120 s) voltage stresses. Except for Fig. 1, which was obtained by AFM topographic scanning, the rest of the images shown in this work

were captured using the optical microscope of the probe station. Data analysis was carried out using the software PASSaGE2 [11]. Although PASSaGE2 has some limitations such as the shape of the structures that can be analyzed, to our knowledge, this is the only software that provides the angular wavelet method as one of its standard point pattern characterization tools.

3. Brief introduction to the angular wavelet method

Angular wavelet analysis is a method developed by Rosenberg [11] for analyzing point pattern distributions. As discussed by Rosenberg, the problem with alternative approaches (directional correlograms, oval templates, 2D spectral analysis) is that they do not determine directions of pattern; they can only be used to test for patterns in *a priori* specified directions. The most recent version of the Spatstat package for the R language, the most popular package for spatial analysis, does not have any wavelet method implemented [12]. A wavelet function $g(x)$ is a scalable function whose integral over all x -values yields zero. The wavelet function describes a kind of template that can be scaled to a given size b_k and shifted to a given location x_i . When the template matches the observed data $y(x_j)$, the value of the wavelet transform W at that location is high, otherwise the value is low (see the scheme in Fig. 2.a). For example, + and – signs in Fig. 2.a indicate good and bad matching of experimental data. The wavelet transform W is defined as:

$$W(b_k, x_i) = \frac{1}{b_k} \sum_{j=1}^n y(x_j) g\left(\frac{x_j - x_i}{b_k}\right) \quad (1)$$

where n is the number of observations. The overall variance for a given position x_i is calculated according to the expression:

$$P(x_i) = \frac{1}{m} \sum_{k=1}^m W^2(b_k, x_i) \quad (2)$$

where m is the total number of discrete measured scales. With this definition, $P(x_i)$ is maximum when the wavelet function corresponding to that position fits the experimental data better than at other positions. For the present analysis the position means the angle measured with respect to the horizontal (east=0°, north=90°). The angular wavelet method has been implemented in [11] and is fundamentally aimed at determining anisotropy effects [13,14].

Briefly, the method considers one of the points in the plot (the focal point), divides the space around it into sectors or quadrats, and counts how many of the other points fall within each sector. These counts are then analysed taking into account that the end sectors wrap around a circle (see Fig. 2.b). Points in opposite quadrats are combined for a single count. At the end, peaks in the variance plot computed using eq.(2) indicate preferred directions in the point pattern. Current version of PASSaGE2 scales the wavelets in the range from 1° to 45° in steps of 1°. In this work, as already mentioned, a global pattern approach is followed, *i.e.* variances are averaged across all possible focal points within a prescribed region of the given point pattern. In other words, the distribution of points is examined from different locations (far from the edges of the structure) and the ensemble of

observations averaged to yield a single value for each angle. In order to show the power of the method, Fig. 3 illustrates an extreme case study in which a Poisson point pattern (Fig. 3.a) and a linear distribution of points (Fig. 3.b) are merged together. Notice the peak in the angular plot corresponding to the introduced anisotropy (Fig. 3.c). In this case, the analysis was restricted to a central region of the pattern (reduced number of focal points) in order to eliminate corner effects and was performed using the Haar wavelet, which is the simplest wavelet template (Fig. 2.c). Of course, for our degraded devices such an extreme situation should not be expected. Our objective is to assess whether the voltage probe affects or not the the final distribution of failure sites and how this deviation is detected in the angular variance plot. This is discussed in the next Section.

4. Results and discussion

As mentioned in Section 2, the devices investigated in this work are Pt/HfO₂/Pt capacitors. They were subjected to ramped, 0→12V (Fig. 4), or constant, 60s,120s@9V (Figs. 5 and 6) voltage stresses. Notice the voltage probe location in each photograph. In order to obtain the best results, the region of analysis has to be selected taken into account the focal points region (usually 20% or 30% of the total area) and the appearance of cross-like features associated with corner effects [13]. The analysis was carried out using Sine wavelets, which are continuous wavelets (see Fig. 2.c). There are no major differences with the Haar wavelet used in the previous Section. The 95% confidence bands (green lines) are also included in the plots and were found by randomizing all data points (100 replications),

including the focal points. In the first example shown in Fig. 4, the cross pattern is almost symmetric (in red) and both diagonals have similar weights (see Fig. 4.c). Since the device was ramped voltage stressed the generation of breakdown spots is a very fast process (instantaneous to the eye) and the resultant number of spots relatively low. This occurs because the current that flows through the structure suddenly increases several orders of magnitude so that a large fraction of the applied bias instantly drops across the series resistance of the device. In this case, the red line is well below the green line which indicates no directional bias. In the second example (Fig. 5), the cross pattern is no longer symmetric but exhibits higher variance peaks in the direction of the voltage probe. The device was constant voltage stressed for 60 s so that the appearance of the BD spots is not instantaneous but sequential. A possible explanation for the observed anisotropy is the occurrence of a kind of feedback effect between the generation of spots (many of them acting as shorts) and the distribution of the current lines in the top electrode. This is confirmed by the case described in Fig. 6. As the device becomes more degraded (120s@9V), with around a thousand of BD spots, the asymmetry of the red cross pattern is still evident with the largest lobes pointing out again in the voltage probe direction (Fig. 6.c). However, the red line is well below the green line which indicates that the directional bias is not so strong. The variance estimator seems to be influenced by the large number of BD spots generated. As it can be seen from the aerial view of the structure (Fig. 6.a), the top electrode exhibits signs of severe degradation directed from the voltage probe

location towards the center of the device, which seems to be the most damaged region of the structure.

In order to confirm these observations using alternative estimators, Fig. 7.a shows a false colour image of a damaged device (450 BD spots). An anomalous large density of spots (blue ellipse) can be seen along the diagonal of the device ($\alpha=0$). The angular probability density function $f(\alpha)$ corresponding to a CSR process in a square region of analysis [3] is indicated by the solid line in Fig. 7.b. In this case, the voltage probe is assumed to be exactly located at one corner of the device (focal analysis). The histogram value at $\alpha=0$ clearly exceeds the expected result for CSR, which indicates accumulation of points in that particular direction. In addition, Fig. 7.c shows that the experimental pair correlation function (derivative of the Ripley's K function) does not match the value corresponding to a CSR process at different distance scales ($g_{CSR}=1$) [4]. The Ripley's K function counts the number of neighboring points found within a given distance of each individual point. Fig. 7.c indicates accumulation of points ($g_{Exp}>1$). From these results, it is clear that the frequent assumption of Poisson distributed BD spots in MIM capacitors should be considered with care and not taken from granted. This hypothesis seems to hold exclusively for low levels of degradation.

5. Conclusions

We showed in this work that the angular wavelets method can be used to investigate the spatial distribution of failure sites in large area MIM capacitors. Although the angular plots are significantly affected by corner effects inherent to

the method, the obtained results for low degradation levels are consistent with isotropic distributions of breakdown spots as expected for Poisson point processes. However, for severely damaged devices some deviations are detected related to preferred directions of degradation associated with the voltage probe location. Importantly, we emphasize that the aim of this work is not to provide a method to locate the source of degradation but to show the effects of some degree of anisotropy in the angular variance plots of BD spots patterns. Finally, it is worth pointing out that the angular wavelet method could be particularly relevant for the reliability assessment of large area electron devices with marks or point defects scattered over their surfaces.

Acknowledgements

This project has received funding from the European Union's Horizon 2020 research and innovation programme under grant agreement No 654384 (Ascent Project Ref. 030 - Tyndall National Institute). This work was also supported in part by the PANACHE EU Project and the DURSI through the Generalitat de Catalunya under Grant 2014SGR384.

References

- [1] C.K. Chui, *An introduction to wavelets. Wavelet analysis and its applications*, Vol. 1, Academic Press, 1992
- [2] M. Dale, M. Mah, J Veg Sci 9, 805-814, 1998
- [3] X. Saura, S. Monaghan, P. K. Hurley, J. Suñé, E. Miranda, IEEE Trans Dev Mat Rel, vol. 14, 1080-1090, 2014
- [4] J. Illian, A. Penttinen, H. Soyan, D. Stoyan, in *Statistical analysis and modelling of spatial point patterns*, Wiley, 2008
- [5] S. Lombardo, J. Stathis, B. Linder, Kin Leon Pey, F. Palumbo, Chih Hang Tung, J Appl Phys, vol. 98, 121301, 2005
- [6] E. Wu, J. Stathis, L. Han, Semicond Sci Technol, vol. 15, p. 425, 2000
- [7] E. Miranda, M. Riccio, G. De Falco, J. Blasco, J. Suñé, A. Irace, J Appl Phys, vol. 115, 174502, 2014
- [8] R. Gallay, Proceedings of the CAS-CERN Accelerator School, Ed. R. Bailey, CERN-2016-003, 45, 2015
- [9] J. Ennis, F. MacDougall, R. Cooper, J. Bates, Power Modulator Symposium, 2002 and 2002 High-Voltage Workshop. Conference Record of the Twenty-Fifth International, 2002, pp. 634–638
- [10] M. Alam, D. Varghese, B. Kaczer, IEEE Trans Elec Dev, vol. 55, pp. 3150-3158, 2008
- [11] M.S. Rosenberg, C.D. Anderson, Methods in Ecology and Evolution, vol. 2, pp. 229-232, 2011

- [12] Package 'Spatstat' for R Language, March 23, 2017, Version 1.50-0.
- [13] M.S. Rosenberg, J Veg Sci, vol. 15, 277-284, 2004
- [14] M. Dale, P. Dixon, M. Forin, P. Legendre, D. Myers, M. Rosenberg, Ecography, vol. 25, 558-577, 2002

Figure captions

1) Image of a typical breakdown spot generated in our devices obtained by AFM scanning.

2) *a)* Schematic of a sequence of experimental data and corresponding wavelet matching Process. The + and - signs indicate positive and negative matching, respectively. *b)* Distribution of angular sectors (quadrants) for a focal point located at the center of the analysis area. Below is the transect created from the sectors indicating circularity. *c)* Mathematical and graphical description of the Haar and Sine wavelets.

3) Example of a superposition of two point patterns. *a)* Poisson point process, *b)* linear distribution of points, and *c)* superposition of Poisson and linear distributions. Notice the peak in the variance plot associated with the presence of the anisotropy. The dashed square indicates the region of focal points.

4) *a)* Distribution of breakdown spots obtained after a ramped voltage stress from 0V to 12V. Notice the presence of the voltage probe close to one edge of the device. *b)* Digital localization of the breakdown events for further processing. *c)* Corresponding angular wavelet variance plot (red line). The green line is the confidence band.

5) *a)* Distribution of breakdown spots obtained after a constant voltage stress at 9 V for 60 s. Notice the presence of the voltage probe close to one corner of the device. *b)* Digital localization of the breakdown events for further processing. *c)* Corresponding angular wavelet variance plot (red line). The green line is the confidence band.

6) *a)* Distribution of breakdown spots obtained after a constant voltage stress at 9 V for 120 s. Notice the presence of the voltage probe close to one corner of the device. Notice the marks on the top electrode of the device associated with severe damage effects. *b)* Digital localization of the breakdown events for further processing. *c)* Corresponding angular wavelet variance plot (red line). The green line is the confidence band.

7) *a)* False color image corresponding to the distribution of failure sites in a severely damaged MIM capacitor. The solid line indicates the diagonal of the device. The blue ellipse points out the BD spots scattered around the diagonal. *b)* The solid line corresponds to the angular probability distribution function for a CSR process. The histogram is found from the experimental data. $\alpha=0$ indicates the diagonal of the device. *c)* Experimental and theoretical (CSR) pair correlation function. The deviation of the experimental curve from unity indicates a non-uniform BD spot distribution.

FIGURES

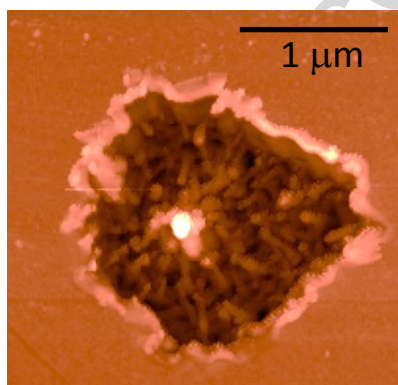


FIGURE 1

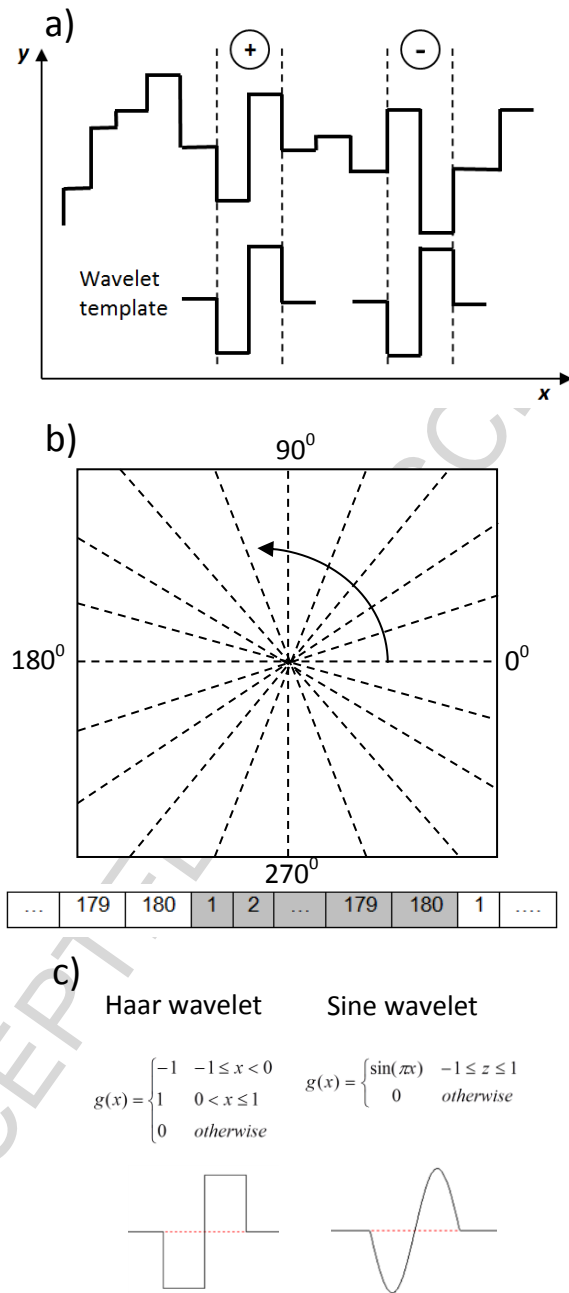


FIGURE 2

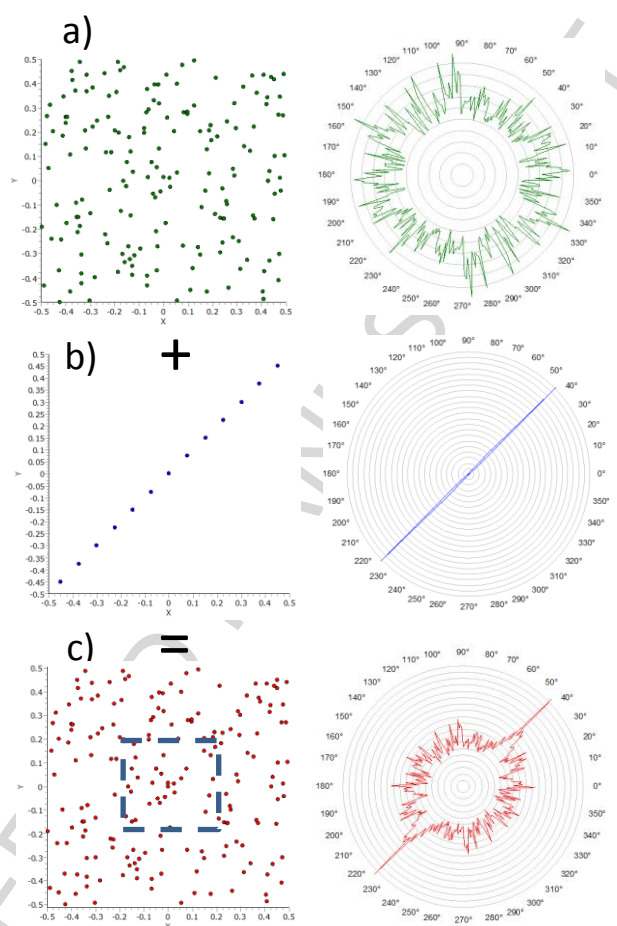


FIGURE 3

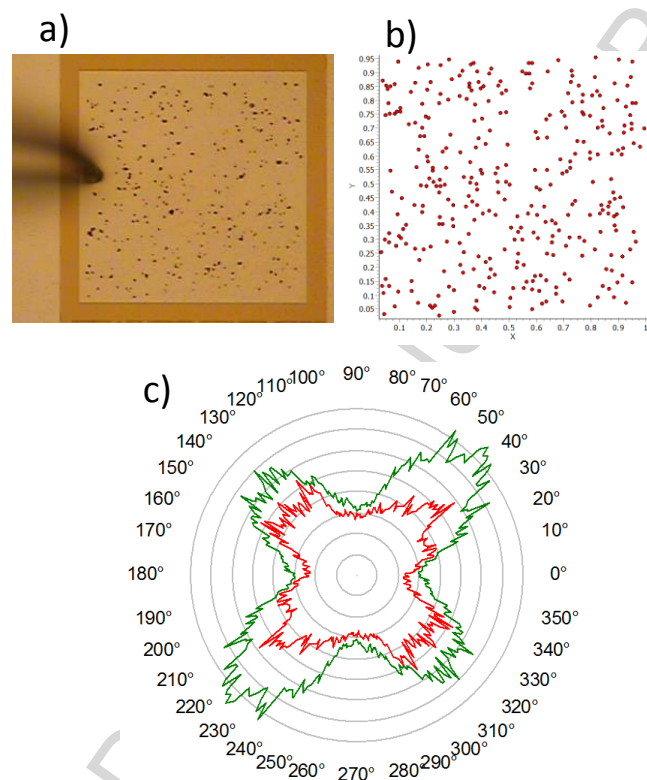


FIGURE 4

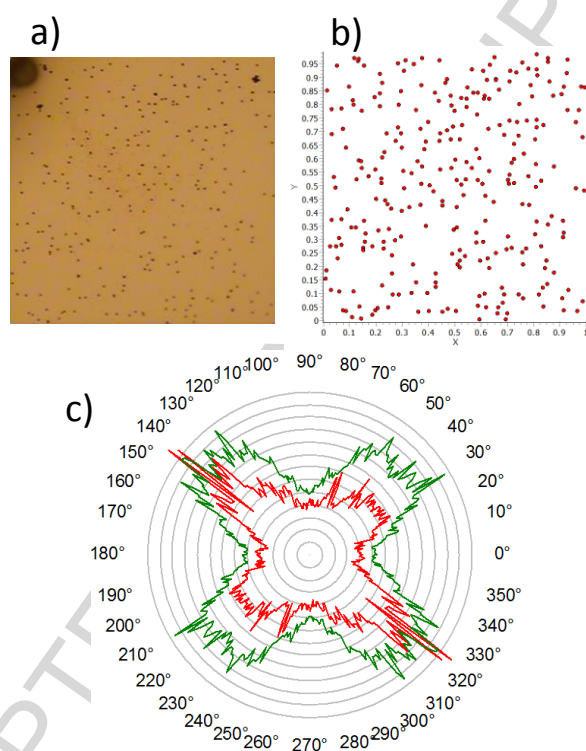


FIGURE 5

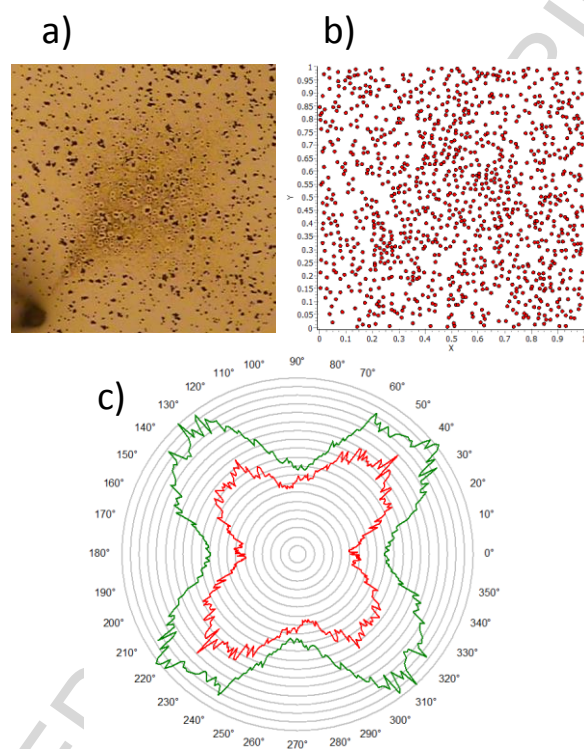


FIGURE 6

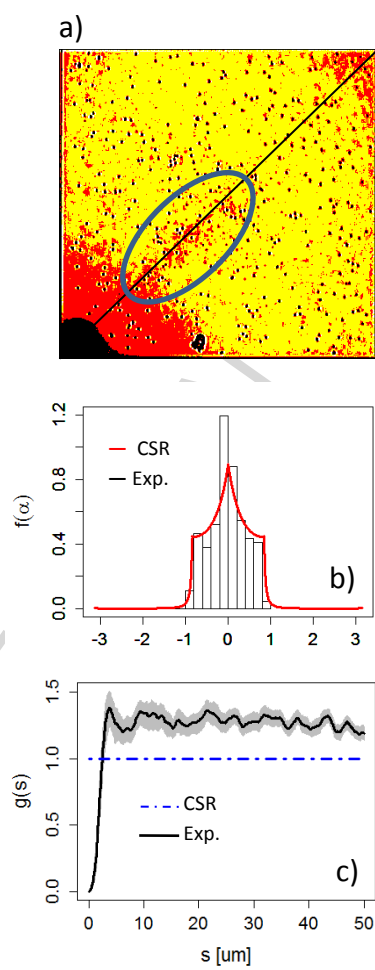
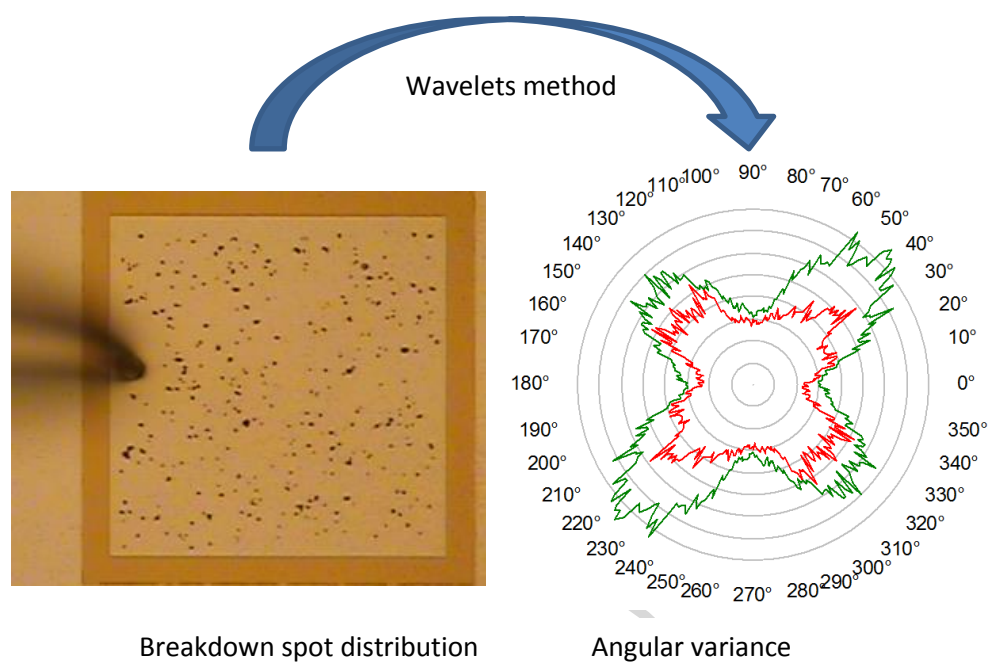


FIGURE 7

Graphical abstract



Highlights

- The spatial distribution of failure sites over the top electrode of a MIM device is investigated
- The analysis is based on the wavelets variance method for the angular distribution
- The effects of anisotropy on the variance induced by the voltage probe location are investigated